

Estimating fishing exploitation rates to simulate global catches of pelagic and demersal fish

Daniel van Denderen¹, Nis Jacobsen¹, Ken H. Andersen¹, Julia L. Blanchard², Camilla Novaglio², Charles A. A Stock³, and Colleen M Petrik⁴

¹Technical University of Denmark

²University of Tasmania

³NOAA Geophysical Fluid Dynamics Laboratory

⁴UC San Diego

March 15, 2024

Abstract

Robust projections of future trends in global fish biomass, production and catches under different fishing scenarios are needed to inform fisheries policy in a changing climate. Trust in future projections, however, relies on establishing that the models used can accurately simulate past relationships between exploitation rates, catches and ecosystem states. Here we use fisheries catch and catch-only assessment models in combination with effort data to estimate regional fishing exploitation levels (defined as the fishing mortality relative to fishing mortality at maximum sustainable yield, $F/FMSY$). These estimates are given for large pelagic, forage and demersal fish types across all large marine ecosystems and the high seas between 1961 and 2004; and with a ‘ramp-up’ between 1841-1960. We find that global exploitation rates for both large pelagic and demersal fish are consistently higher than for forage fish and reached their peaks in the late 1980s. We use the exploitation rates to globally simulate historical fishing patterns in a mechanistic fish community model. We find a good match between model and reconstructed fisheries catch, both for total catch as well as catch distribution by functional type. Simulations show a clear deviation from an unfished model state, with a 25% reduction in fish biomass in large pelagic and demersal fish in shelf regions in the most recent years and a 50% increase in forage fish, primarily due to the release of predation pressure. These results can set a baseline from which the effect of climate change relative to fishing could be estimated.

Hosted file

Manuscript_submission.docx available at <https://authorea.com/users/572236/articles/723364-estimating-fishing-exploitation-rates-to-simulate-global-catches-of-pelagic-and-demersal-fish>

Hosted file

Supplement_submission.docx available at <https://authorea.com/users/572236/articles/723364-estimating-fishing-exploitation-rates-to-simulate-global-catches-of-pelagic-and-demersal-fish>

1

2 **Estimating fishing exploitation rates to simulate global catches of pelagic and**
3 **demersal fish**

4 **P. D. van Denderen^{1,2}, N. Jacobsen¹, K. H. Andersen¹, J.L. Blanchard^{3,4}, C. Novaglio^{3,4}, C.**
5 **A. Stock⁵, C. M. Petrik⁶**

6 ¹DTU Aqua, Technical University of Denmark, Lyngby, Denmark.

7 ²Graduate School of Oceanography, University of Rhode Island, Narragansett, Rhode Island,
8 USA

9 ³Institute for Marine and Antarctic Studies, University of Tasmania, Hobart, Tasmania, Australia

10 ⁴Centre for Marine Socioecology, University of Tasmania, Hobart, Tasmania, Australia

11 ⁵Geophysical Fluid Dynamics Laboratory, NOAA, Princeton, New Jersey, USA

12 ⁶Scripps Institution of Oceanography, University of California, San Diego, California, USA

13

14 Corresponding author: Daniel van Denderen (pdvd@aqua.dtu.dk)

15

16 **Key Points:**

- 17 • estimated global gridded fishing exploitation patterns for large pelagic, forage and
18 demersal fish types using catch and effort data
19
- 20 • food-web simulations broadly replicated catch trends of diverse ecosystems on a global
21 scale
- 22
- 23 • found global biomass declines due to fishing in large pelagic and demersal fish and
24 increases in forage fish due to a trophic cascade

25 Abstract

26 Robust projections of future trends in global fish biomass, production and catches under different
27 fishing scenarios are needed to inform fisheries policy in a changing climate. Trust in future
28 projections, however, relies on establishing that the models used can accurately simulate past
29 relationships between exploitation rates, catches and ecosystem states. Here we use fisheries
30 catch and catch-only assessment models in combination with effort data to estimate regional
31 fishing exploitation levels (defined as the fishing mortality relative to fishing mortality at
32 maximum sustainable yield, F/F_{MSY}). These estimates are given for large pelagic, forage and
33 demersal fish types across all large marine ecosystems and the high seas between 1961 and 2004;
34 and with a 'ramp-up' between 1841-1960. We find that global exploitation rates for both large
35 pelagic and demersal fish are consistently higher than for forage fish and reached their peaks in
36 the late 1980s. We use the exploitation rates to globally simulate historical fishing patterns in a
37 mechanistic fish community model. We find a good match between model and reconstructed
38 fisheries catch, both for total catch as well as catch distribution by functional type. Simulations
39 show a clear deviation from an unfished model state, with a 25% reduction in fish biomass in
40 large pelagic and demersal fish in shelf regions in the most recent years and a 50% increase in
41 forage fish, primarily due to the release of predation pressure. These results can set a baseline
42 from which the effect of climate change relative to fishing could be estimated.

43

44 Plain Language Summary

45 Fishing can heavily impact the number and types of fish in a region. Yet, simulating the
46 historical impacts of fishing on fish communities is challenging, especially on a global scale.
47 This is because for many places, we do not know how many fish are in the sea and what fraction
48 of these fish die from fishing each year. In this study, we estimated the historical rate by which
49 fisheries have caught fish globally. We used these data in a mathematical model to simulate the
50 number of fish in the sea; both with and without fishing. The model shows that fishing has
51 reduced the biomass of big predators (large pelagic and demersal fish) with 25% in shelf regions.
52 This decline led to less predation on forage fish and a 50% increase in forage fish biomass,
53 despite forage fish fisheries. These simulations provide a starting point for estimating the relative
54 effects of climate change and fishing on future fish communities.

55 **1 Introduction**

56 Marine capture fisheries contribute to global food security with landings of 90 million
57 metric tonnes annually in the last decades (FAO, 2022; Watson, 2017). Fisheries operations
58 support employment and trade but have also caused global concerns about the impacts of fishing
59 on individual populations of harvested species, fish communities and the structure and function
60 of the ecosystem (Jennings & Kaiser, 1998; Myers & Worm, 2003). Historical simulations of
61 fish biomass and fisheries production are important to describe how and why the oceans have
62 changed due to fisheries. In addition, these simulations can provide a baseline of fish biomass
63 under current exploitation rates to support assessments of climate change impacts on fisheries
64 and marine ecosystems (Blanchard et al., this issue).

65 Marine ecosystem models of upper trophic level organisms, hereafter termed MEMs,
66 have been used to simulate historical fish community biomass (Bianchi et al., 2023; Blanchard et
67 al., 2012; Christensen et al., 2015; Galbraith et al., 2017; Petrik et al., 2019). MEMs typically
68 require instantaneous fishing mortality rates to simulate fish catches and changes in fish biomass
69 with fishing. MEMs have faced challenges in parameterizing the effects of fishing due to
70 uncertainty in fishing exploitation levels for fish populations, functional types and communities
71 in most national waters and the high seas. As a result, some MEMs have used a fishing mortality
72 rate that approximates model estimated maximum sustainable yield (MSY) and compared these
73 to observational estimates of peak catches in historically fished ecosystems (Blanchard et al.,
74 2012; Petrik et al., 2019). Other MEMs, simulating historical fishing catches over time, have
75 adopted approaches that translate fishing effort, often measured by engine power and days at sea,
76 to fishing mortality and catch and use bootstrapping to find a set of model parameters that
77 produce the best agreements with observed fish catches (Christensen et al., 2015; Galbraith et al.,
78 2017). In such approaches, estimating model parameters that relate to fishing processes can be
79 challenging and computationally expensive for complex MEMs, that may require multiple
80 fishing mortality estimates per year and spatial domain. Furthermore, many regional-scale
81 MEMs take fishing mortality rates as direct input rather than fishing effort (SI in Blanchard et al.
82 this issue). However, existing fishing mortality estimates are often based on single-species stock
83 assessments for particular regions, e.g. Jacobsen et al. (2017), and not available across regions
84 and functional types. Thus standardized data on fishing mortality rates for different regions of
85 the world, required for systematic model intercomparison projects (such as the Fisheries and
86 Marine Ecosystem Model Intercomparison Project, FishMIP) of fishing impacts, are currently
87 lacking.

88 Catch-only stock assessment models combine time series of catch with population
89 dynamic models to estimate stock status in cases where data is limited and estimates of stock
90 abundance are unavailable (Froese et al., 2017; Thorson et al., 2012). Despite that catch-only
91 models can lead to biased estimates of stock status and poor management advice (Bouch et al.,
92 2021; Free et al., 2020; Ovando et al., 2021), they are an effective means of assessing stock
93 status for the majority of global fisheries that lack sufficient data for formal stock assessments.
94 Catch-only models may thus, in the context of global and regional model intercomparison
95 projects, offer a transparent way to externally estimate the rate at which fish biomass is caught,
96 i.e. the fishing mortality rate, for a large range of ecosystems and fish types. Fishing mortality
97 rate estimates could usefully serve as standardized inputs to MEMs to simulate fish catches and
98 historical changes in biomass, where observational estimates of fisheries catches and biomass
99 may be used for model validation (Blanchard et al., this issue).

100 In this study, we used catch-only stock assessment models to estimate a time series of
101 fishing mortality (F) relative to the fishing mortality that supports maximum sustainable yield
102 (F_{MSY}) per Large Marine Ecosystem (LME) for three fish functional types: forage fish, large
103 pelagic fish, and demersal fish. We focused on obtaining an F/F_{MSY} time series, rather than an F
104 time series, as the F/F_{MSY} time series provides a forcing usable in most MEMs, where F_{MSY}
105 depends on each MEM's specifications and assumptions. For all LMEs with intermediate and
106 high catches, the F/F_{MSY} time series was estimated from time series of fisheries landings
107 (Watson, 2017). For low catch LMEs and the high seas, the time series was estimated by
108 combining global effort data with the F/F_{MSY} estimates from the intermediate and high catch
109 LMEs. We allocated the estimated F/F_{MSY} per functional type, ecosystem, and year across a 0.5-
110 degree spatial grid in proportion to total gridded effort in each ecosystem (Rousseau et al., 2022,
111 2024). We used the gridded estimates to simulate historical fishing intensity between 1961 and
112 2004 with the Fisheries Size and Functional Type model, FEISTY (Petrik et al. 2019). We
113 compared the model simulations of FEISTY with observational estimates of fisheries landings in
114 the same period. We then evaluated the simulated global changes in fish biomass as compared to
115 an unfished ocean.

116 2 Methods and Data

117 2.1 Method summary

118 We utilized data from three distinct data sources to construct a time series of F/F_{MSY} per
119 LME (including the high seas as one region), spatially allocated across a 0.5-degree spatial grid,
120 for demersal, large pelagic, and forage fish. These data sources encompassed: 1) a global catch
121 reconstruction aggregated by functional type and LME (including the high seas as one region)
122 from 1961 to 2004, 2) nominal fishing effort data by functional type and LME (including the
123 high seas as one region) between 1841 and 2004, and 3) total nominal fishing effort data gridded
124 at a 0.5-degree spatial resolution from 1961 to 2004. These data products were prepared by
125 FishMIP as part of the Intersectoral Model Intercomparison Project (ISIMIP) and are available at
126 isimip.data.org, see Blanchard et al. this issue and Frieler et al. (2023) for further details.

127 We estimated an F/F_{MSY} timeseries using a data limited catch assessment model (see
128 section 2.3) for all LME \times functional type combinations with intermediate and high catches (see
129 definitions below). For all remaining combinations and the high seas, we converted the nominal
130 effort time series per functional type to an F/F_{MSY} timeseries using conversion factors from the
131 intermediate and high catch LMEs (see section 2.4). The F/F_{MSY} values were then allocated per
132 year across a 0.5-degree spatial grid in proportion to total gridded effort in each LME/high seas.
133 To exemplify how the gridded F/F_{MSY} data set can be input into MEMs to generate historical
134 time series of fish biomass and catch, they were input into the FEISTY model forced by outputs
135 from GFDL's ocean model (MOM6-COBALTv2) (Adcroft et al., 2019; Stock et al., 2020) that
136 provides monthly means of physics, biogeochemistry, and lower trophic level production
137 (section 2.5). The ocean model simulations were run on a 0.25-degree spatial grid using
138 boundary condition forcing from the Japanese 55-year Reanalysis (JRA-55) products (Tsuji no et al., 2018) and temporally dynamic river freshwater and nitrogen fluxes (Liu et al., 2021). Ocean
139 model outputs were interpolated to a regular 1-degree grid for the FishMIP contribution to the
140 ISIMIP Phase 3a protocol (Blanchard et al. this issue) and interpolated to a daily time step for
141 coupling with FEISTY. We ran scenarios both with and without fishing and compared the
142 modeled fishing catch with reconstructed catch.
143

144 2.2 Catch and Effort Data

145 Fisheries catch, estimated as the sum of reported landings, illegal, unreported and
 146 unregulated catch and discards, were aggregated per functional type and LME for the period
 147 1961-2004 from gridded catch data (Watson, 2017; Watson & Tidd, 2018). The demersal fish
 148 functional type included all species that were classified in Watson (2017) as demersal, bentho-
 149 pelagic, flatfish, reef-associated and bathydemersal. Forage fish included all fish classified in
 150 Watson (2017) as pelagic fish < 30 cm and large pelagic fish included all fish classified as
 151 pelagic fish > 30 cm. All other fisheries catch types, representing 17% of total catch, were not
 152 simulated in this study. Total industrial and artisanal fishing effort data by functional type and
 153 LME (including the high seas as one region) were aggregated from Rousseau et al. (2022, 2024)
 154 and then reconstructed for the period 1861-2004 using generalised additive models (SI of
 155 Blanchard et al. this issue). The data describe nominal effort of the active fleet based on the
 156 engine power of the active fleet multiplied with the average days at sea of one vessel. Gridded
 157 total industrial and artisanal fishing effort, on a 0.5-degree spatial resolution, for the period 1961-
 158 2004 were obtained from Rousseau et al. (2022, 2024).

159 2.3 Catch-only Assessment Model

160 We applied the Catch-MSY model (Martell & Froese, 2013) to estimate the relative
 161 historical fishing pressure in each of the LMEs. First, we modified the standard Schaefer
 162 formulation to the Pella-Tomlinson formulation of surplus production to be able to attribute
 163 different shape parameters to each of the functional types:

$$164 B_{i,t+1} = B_{i,t} + \frac{r_i}{(n_i-1)} B_{i,t} \left(1 - \frac{B_{i,t}}{K_i} \right)^{n_i-1} - F_{i,t} B_{i,t},$$

165 where B is the exploited biomass of functional type i , n is a shape parameter determining at
 166 which fraction of the unfished biomass MSY occurs, r is the population growth parameter, and K
 167 is the carrying capacity. We used the catch information as input data to infer the fishing mortality
 168 as $C_{i,t} = F_{i,t} B_{i,t}$. We *a priori* assigned n for each of the functional types before assessing the
 169 past F/F_{MSY} status using the n estimates from Thorson et al. (2012) (Table 1), who estimated the
 170 shape parameters based on an analysis of 147 data rich stocks in the RAM stock assessment
 171 database. The fit was conducted by testing a set of r - K combinations which gave a realistic
 172 historical biomass distribution. Here realistic is defined as the biomass always being above 0 and
 173 below the carrying capacity (which only works for fished stocks). We then used the median r - K
 174 combinations to recreate the historical biomass distribution and consequently calculate the
 175 estimated $B_{i,t}$. We used the estimates to calculate $MSY_i = \frac{rK}{n^{n-1}}$, and $F_{MSY} = \frac{MSY}{n \left(\frac{1}{1-n} \right)^K}$ and visually
 176 inspected fits to ensure that the MSY estimates were within reasonable boundaries considering
 177 the past catches.

178

179

180

181

182

183

184 **Table 1.** Shape parameters for the three fish functional types in the Catch-MSY model.

185

Functional type	<i>n</i>
Demersal	1.540
Small pelagics	0.599
Large pelagics	1.431

186

187 The catch-only assessment model performs best when the catch time series covers a
 188 period where fishing catches have a large degree of contrast, *i.e.*, both fishing above and below
 189 MSY. Consequently, we excluded certain LMEs with historically low fishing exploitation from
 190 the catch assessment analysis. Specifically, we excluded the Arctic and Antarctic systems, most
 191 Australian LMEs and the insular Pacific-Hawaiian LME, following Stock et al. (2017), and the
 192 high seas. Furthermore, in some LMEs with intermediate and high total catch, certain functional
 193 types exhibited low catches. We thus removed any functional type that contributed less than 5%
 194 to the total catch within a given LME. These exclusions resulted in an estimate of F/F_{MSY} in 45
 195 LMEs for demersal and large pelagic fish and 34 LMEs for forage fish. We compared the F/F_{MSY}
 196 time series of several LMEs and functional types with stock assessment time series of F/F_{MSY}
 197 obtained from the Ram Legacy database v4 (RAM Legacy Stock Assessment Database, 2018)
 198 and the ICES Stock Assessment Graphs database (downloaded January 2023). The comparison
 199 was done for 135 stocks that were aggregated in 14 LME \times functional type combinations
 200 (Supplementary Figure S1).

201 2.4 Time series of F/F_{MSY} per grid cell

202 The F/F_{MSY} time series from the catch assessment model only provides information for
 203 functional types in intermediate and high catch LMEs for 1961-2004. For each of these LME \times
 204 functional type combinations, we estimated F/F_{MSY} time series for 1841-1960 using the nominal
 205 effort time series per functional type and LME and factors that convert nominal effort to F/F_{MSY} .
 206 To this end, we selected from each catch assessment model outcome the five years closest to
 207 F_{MSY} and MSY. We paired these selected years per functional type and LME with the nominal
 208 effort and averaged the nominal effort values. This average value approximates the total nominal
 209 effort per year that is needed to fish a functional type at F_{MSY} in an LME. We standardized these
 210 nominal effort values to nominal effort at F_{MSY} per km² by dividing by the areal extent of the
 211 fished part of each LME. The fished part was estimated using the total gridded effort information
 212 and by selecting all grid cells (sorted from high to low effort) that correspond to 95% of total
 213 effort in each LME. The standardized nominal effort at F_{MSY} served as the conversion factors to
 214 compute F/F_{MSY} time series for functional types in intermediate and high catch LMEs between
 215 1841-1960 assuming a linear relationship between effort and mortality. In addition, we used the
 216 conversion factors to estimate F/F_{MSY} time series for 1841-2004 for functional types in all low
 217 catch LMEs and the high seas. This was done by converting the time series of nominal effort per
 218 functional type and LME to an F/F_{MSY} time series using a conversion factor from an adjacent
 219 area or the global median of a functional type (Supplementary Table S1).

220 The spatial allocation of fishing mortality for each functional type to each 0.5-degree grid
 221 cell was done in proportion to total gridded effort in each LME. For the period 1961-2004, the
 222 allocation was based on the existing annual information. For the period 1841-1960, we kept the
 223 spatial allocation the same as for the year 1961.

224 2.5 Mechanistic fish community model FEISTY

225 FEISTY is a temporally dynamic, spatially explicit, mechanistic model that simulates the
 226 biomasses of forage fish (small pelagics), large pelagic, and demersal fishes (Petrik et al. 2019).
 227 Fish functional types are defined by their maximum size, habitat, and prey preferences. Both
 228 large pelagic and forage fish feed on prey, fish and/or zooplankton, in the pelagic zone
 229 throughout their life. Demersal fish initially feed in the pelagic and then transition to the benthic
 230 zone as juveniles at 0.5 g. Demersal fish >250 g feed as generalists on both pelagic and benthic
 231 resources in shelf areas <200 m depth, whereas they feed solely in the benthic zone in deeper
 232 areas. FEISTY includes a multi-stage life cycle of these fishes and includes food-dependent
 233 growth and reproduction. All metabolic and feeding rates scale with individual body size.
 234 Maturation is modeled with a food-dependent function that translates individual-level
 235 assumptions about growth in body size to the population level (de Roos et al., 2008). Growth,
 236 reproduction, and mortality are the consequence of prey encounter and consumption, standard
 237 metabolism, predation, and fishing, which depend on (1) habitat temperatures that affect the
 238 speed of rates, (2) mesozooplankton biomass, mesozooplankton loss rates to higher predators,
 239 and detritus flux to the seafloor that set the food available to upper trophic levels, (3) explicit
 240 predator-prey interactions and competition. FEISTY has been reasonably successful in
 241 representing observed trends of peak fisheries catches (correlation between observed and
 242 modeled total catch per LME is 0.54) and reproduces the underlying mechanisms involved in
 243 structuring large pelagic vs. demersal fish (Petrik et al. 2019).

244 In past simulations when FEISTY was coupled to outputs from COBALT (Petrik et al.
 245 2019, 2020), forcings included distinct medium and large zooplankton groups (small and large
 246 mesozooplankton). The simulations here were completed using the FishMIP protocol (Blanchard
 247 et al. this issue) that combines the COBALT medium and large zooplankton into one
 248 mesozooplankton group. Additionally, zooplankton loss rates to higher predators Z_{HPloss} are not
 249 provided. Thus an empirical relationship between mesozooplankton biomass z_{bio} and upper water
 250 column temperature T_{pel} was developed to estimate these rates as successfully used in past
 251 FishMIP simulations (Heneghan et al., 2021; Tittensor et al., 2021):
 252 $Z_{HPloss} = 10^{(-2.925 + 1.964 \cdot \log_{10}(z_{bio} + eps))} + 1.958 \cdot 10^{-2} \cdot T_{pel}$, with eps being a value close to
 253 zero.

254 2.5 Model parameterization and simulations

255 All FEISTY model parameters were taken from Petrik et al. (2019). We implemented
 256 fishing in FEISTY from the F/F_{MSY} time series by identifying the fishing mortality that
 257 corresponds to F_{MSY} in FEISTY. F_{MSY} is a dynamic parameter that varies with the food web
 258 configuration, the amount of fishing on the other fish types, fishing selectivity, as well as the
 259 abiotic conditions. Finding F_{MSY} for each permutation of these factors was computationally
 260 prohibitive. Instead, we examined how F_{MSY} varied with prey production and temperature for
 261 large pelagic and demersal fish (Supplementary Figure S2; no such estimation could be made for
 262 forage fish as they are heavily depending on fish predation mortality). We found that changes in
 263 prey production had a limited effect on F_{MSY} , but temperature had a large predictable effect
 264 resulting from a higher turnover rate of biomass in FEISTY in warmer waters, which makes fish
 265 more resilient to fishing. We thus approximated the temperature effect on F_{MSY} in FEISTY with

266 a temperature term that is linked to the thermal sensitivity of metabolism ($0.063 \text{ }^\circ\text{C}^{-1}$). We set the
 267 daily fishing mortality F for each functional type f , including forage fish, as:

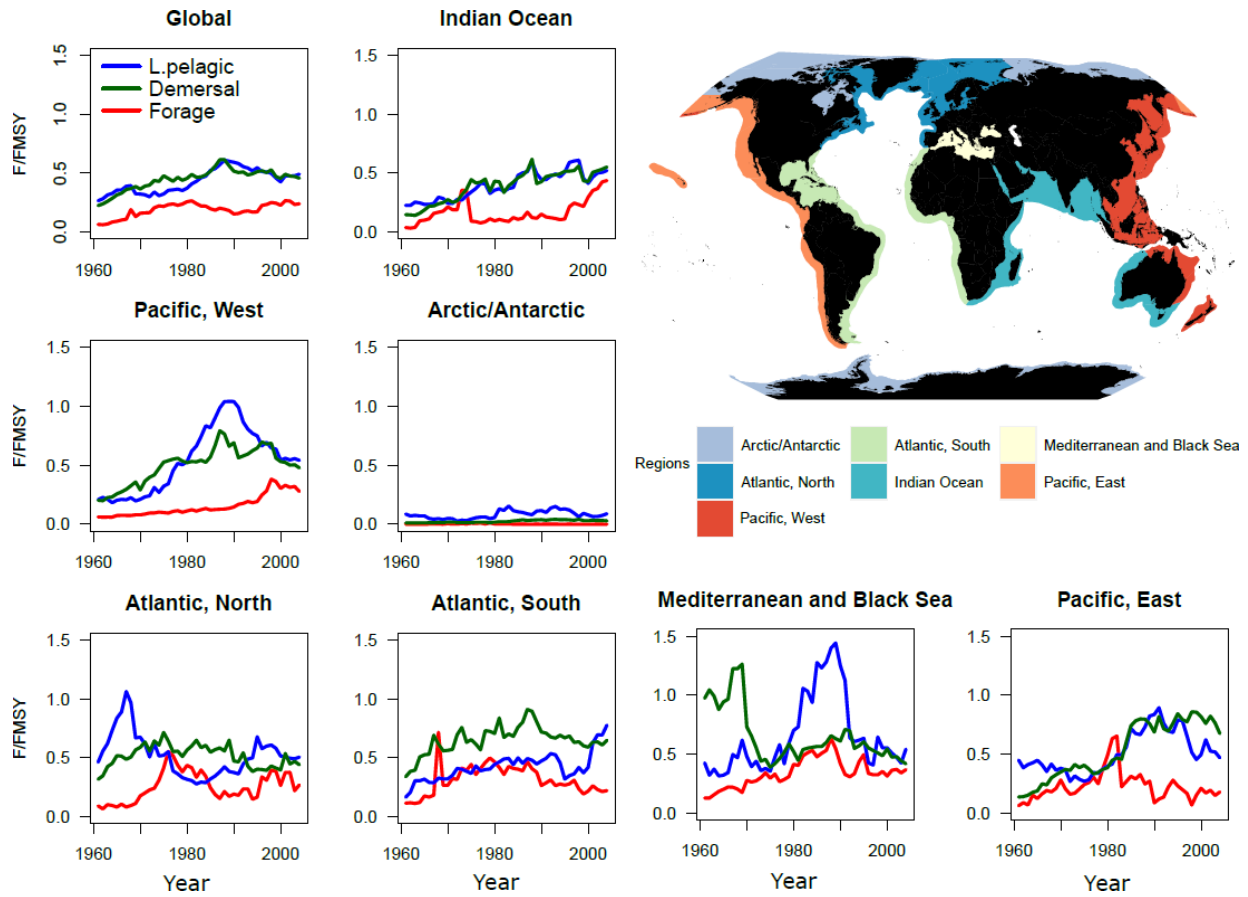
$$F_{i,f,t} = \frac{0.3}{365} \cdot \left(\frac{F}{F_{MSY}}\right)_{i,f,t} \cdot \exp\left(0.063 \cdot (T_{i,t} - 10)\right)$$

268 where T ($^\circ\text{C}$) is the mean habitat temperature in grid cell i and day t ($T = 0$ -100m mean for
 269 forage fish and large pelagics and $T =$ bottom temperature for demersal fish), 0.3 is the obtained
 270 value of F_{MSY} in FEISTY at $10 \text{ }^\circ\text{C}$, and $(F/F_{MSY})_{i,f,t}$ is based on the time series derived as
 271 described in the prior section. Fishing gear selectivity was 100% for the largest size class of all
 272 functional types ($1 \times F_{i,f,t}$). In addition, large pelagic and demersal fish were fished with 10%
 273 selectivity at the juvenile stage ($0.1 \times F_{i,f,t}$). Model spin-up with the ocean-forcing variables and
 274 fishing mortality was done by repeating cycles of the ocean inputs between 1961-1980 (there are
 275 no ocean outputs prior to 1961) combined with the fishing mortality of 1841. We afterwards ran
 276 the model with daily time steps from 1841 up to 2004 using year-specific fishing mortalities
 277 from 1841 and year-specific ocean outputs from 1961. In addition, we ran FEISTY without
 278 fishing as an alternate scenario

279 **3 Results**

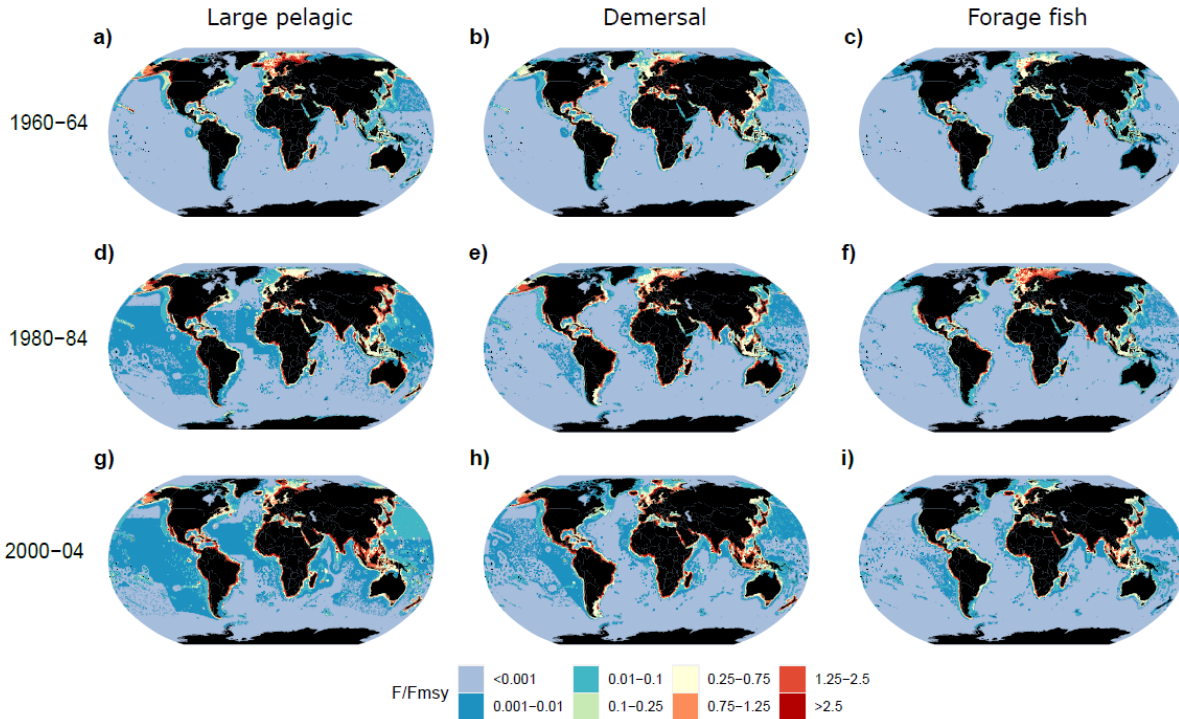
280 3.1 Fishing exploitation patterns

281 Large pelagic and demersal fish are, on average, fished with a higher intensity than
 282 forage fish (Figure 1). On a global scale, both large pelagic and demersal fish peak in
 283 exploitation rate in the late 1980s, but the exploitation patterns strongly vary between regions.
 284 The Arctic/Antarctic region has the lowest exploitation for all fish types and the Mediterranean
 285 and Black Sea region the highest. Large pelagic fishing intensity peaks in the North Atlantic
 286 before the 1970s and in the Eastern and Western Pacific and Mediterranean and Black Sea
 287 around the 1990s. Large pelagic fishing intensity is highest in the South Atlantic and Indian
 288 Ocean in the most recent years. Demersal fishing intensity peaks in the Mediterranean and Black
 289 Sea region before the 1970s. Demersal fishing intensity is relatively constant, with F/F_{MSY}
 290 around 0.6, in the North and South Atlantic and Western Pacific between 1970s and 2000s.
 291 Demersal fishing intensity is highest in the Indian Ocean and Eastern Pacific in the most recent
 292 years. For forage fish, the patterns are more variable, but most regions have a peak in forage fish
 293 fishing mortality in the 1980s and/or the 2000s.



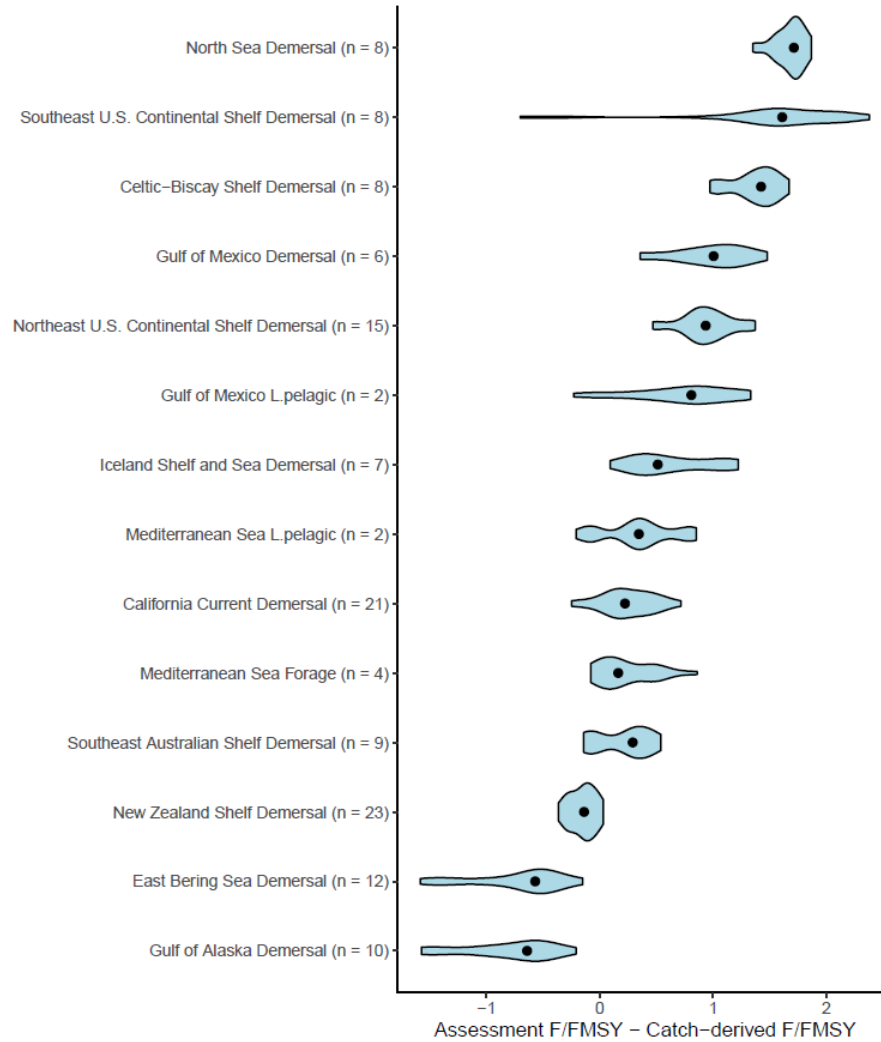
294
 295 **Figure 1.** Time series of average annual exploitation rates (F/F_{MSY}) aggregated per region based
 296 on the average of all LMEs in each region (all LMEs are given equal weight).
 297

298 Maps of the gridded exploitation patterns mirror the above results (Figure 2). The maps
 299 show that most LMEs with a narrow shelf have a relatively high F/F_{MSY} in the shallow areas and
 300 low values in the deeper regions. This distribution reflects the spatial allocation of fishing
 301 intensity in proportion to total gridded effort in each LME (see method). Large pelagic fish are
 302 fished at higher intensity in the high seas than demersal and forage fish.



303
 304 **Figure 2.** Maps of gridded average F/F_{MSY} for large pelagic (a, d, g), demersal (b, e, h) and
 305 forage fish (c, f, i) in the early 1960s, 1980s and 2000s.

306 A comparison between F/F_{MSY} from data-rich stock assessments and the catch-derived
 307 F/F_{MSY} shows that the catch-derived F/F_{MSY} is comparable to but on average lower than the
 308 stock-derived F/F_{MSY} (Figure 3 & S1). Part of this difference may be attributed to the selection of
 309 species; the stock assessment data consist of the most important fished species, whereas the
 310 catch-derived estimates are based on the whole community catch. Nevertheless, it is likely that
 311 the catch-derived assessment has underestimated fishing mortality in some regions. The reverse,
 312 an overestimation of fishing mortality, happened in the Eastern Bering Sea and the Gulf of
 313 Alaska (Figure 3).



314

315 **Figure 3.** Violin plots with annual differences between stock assessment F/F_{MSY} and catch-only
 316 derived F/F_{MSY} for 14 LME \times functional type combinations between 1980 and 2004. The stock
 317 assessment F/F_{MSY} are based on the geometric mean (equal weighting of each stock). The dot
 318 shows the median difference. A difference of 1 (-1) indicates that the assessment-derived F/F_{MSY}
 319 is one F_{MSY} higher (lower) than the catch-derived. See supplementary Figure S1 for individual
 320 time-series of each stock.

321

3.2 Simulations of fish catch

322

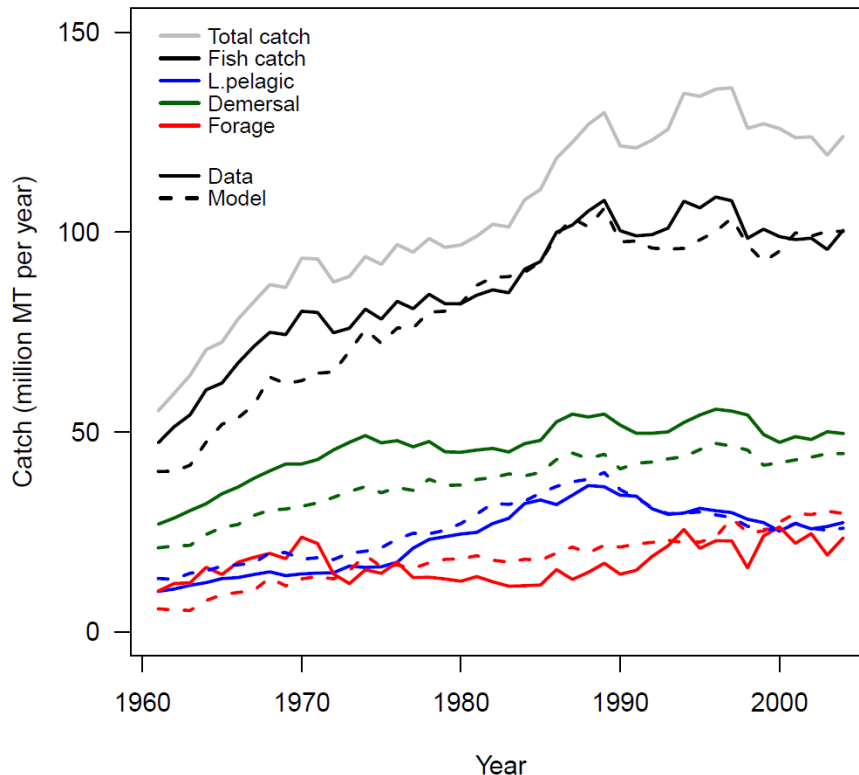
323

324

325

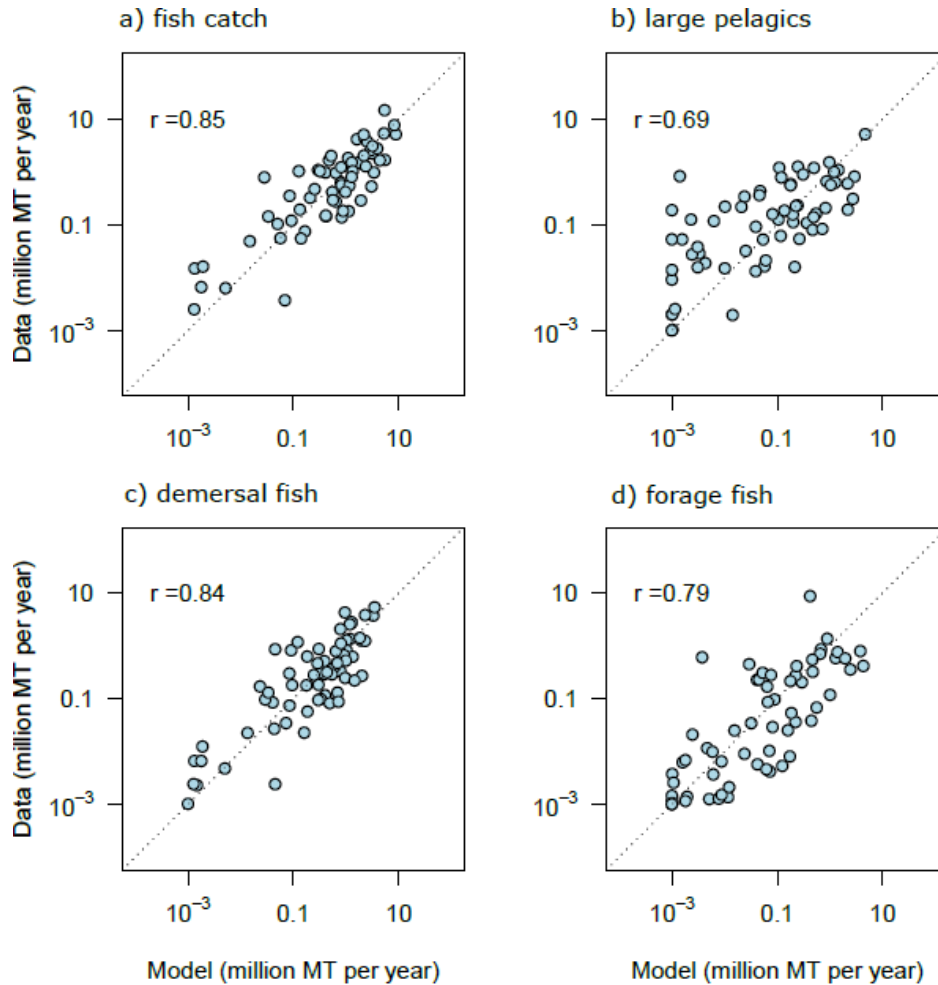
326

Simulated time series of global catches derived by applying the F/F_{MSY} estimates above to FEISTY show good agreement with reconstructed fisheries catches, especially for total fish and large pelagic fish catch (Figure 4). Model estimates of demersal fish are typically 5 to 10 million metric tonnes per year lower. Forage fish modeled catches are close to the fisheries catch data but show a steady increase over time which is not observed in the data.



327
 328 **Figure 4.** Time-series of observed (solid) versus model-based (dashed) catches. Fish catch
 329 includes all fish classified as large pelagic, forage fish and demersal in our study. Total catch
 330 includes all marine organisms and was not simulated in the study.

331
 332 Comparisons of observed and modeled fish catches across LMEs show a high correlation
 333 for total landings ($r = 0.85$), demersal fish ($r = 0.84$) and forage fish (0.79) (Figure 5). Large
 334 pelagic fish have a correlation of 0.69 and lower modeled catches in several LMEs, among
 335 others, the Sulu-Celebes Sea and the Northeast Australian Shelf. In absolute numbers, the
 336 difference between model and data in total landings is less than $1 \text{ million MT y}^{-1}$ in 78% of the
 337 LMEs. In addition, no consistent mismatch in catch is observed for specific latitudinal regions.
 338 The largest differences between data and model are observed in the Humboldt Current (9.4
 339 million MT y^{-1} higher in data mainly due to forage fish catch), Mediterranean Sea (3.8 million
 340 MT y^{-1} higher in model), Arabian Sea (3.6 million MT y^{-1} higher in model) and Sea of Okhotsk
 341 (2.9 million MT y^{-1} higher in data).



342
343

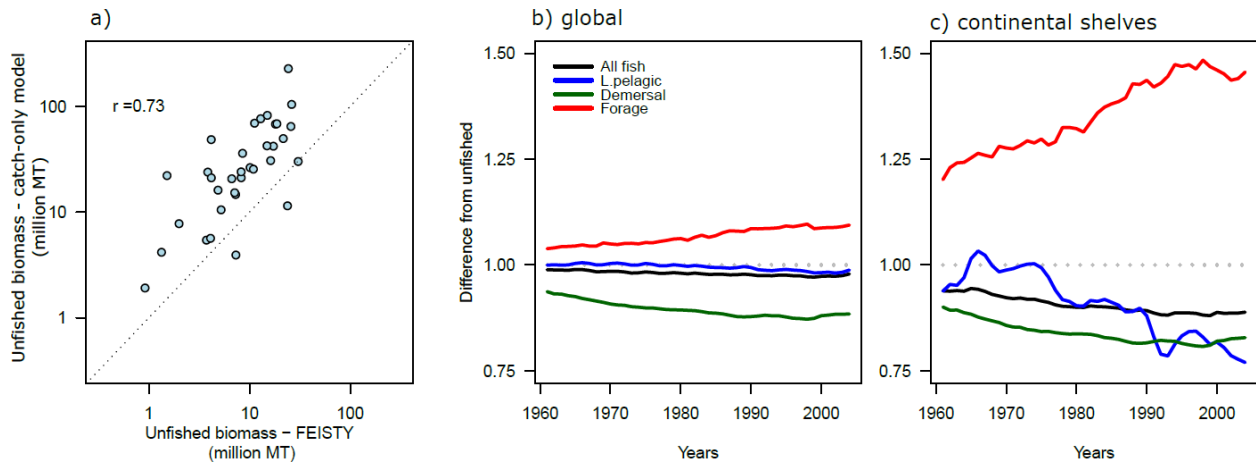
344 **Figure 5.** Comparison of observed and modeled fish catch per LME based on the mean catch
345 between 1990-2000. Fish catch (a) includes all fish classified as large pelagic (b), demersal (c)
346 and forage fish (d) in our study. A value of 0.001 million MT was added to both data and model
347 outputs to limit focus on very low catches.

348 3.3 Simulations of fish biomass

349 Global fish biomass in the unfished scenario is varying between 1.72 and 1.85 gigaton in
350 the period 1961-2004. Simulated unfished biomass is typically lower than the estimated unfished
351 biomass (parameter K) derived from the catch-only model for LMEs with intermediate and high
352 catches, though positively correlated (Figure 6a, and supplementary Figure S3 for each
353 functional type). Relative to an unfished scenario, fishing has resulted in a global biomass
354 decline of 10-15% in large pelagic and demersal fish and 25% decline in shelf regions as of 2004
355 (Figure 6b-c). In contrast, the simulations show a global increase of 25% in forage fish biomass
356 in the fishing scenario and a 50% increase in shelf regions, primarily caused by the release of
357 predation pressure from large demersal and pelagic fish. Demersal fish show a clear decline in
358 biomass with increasing fishing pressure across LMEs. Demersal fish biomass is around 60% of
359 the unfished biomass in LMEs that are fished at F_{MSY} (Figure 7b). The biomass response of large
360 pelagics and forage fish across LMEs is largely unrelated to fishing pressure on each of these

361 types (Figure 7a and c), suggesting that the biomass changes in these groups are strongly
 362 impacted by trophic interactions beyond fishing.

363



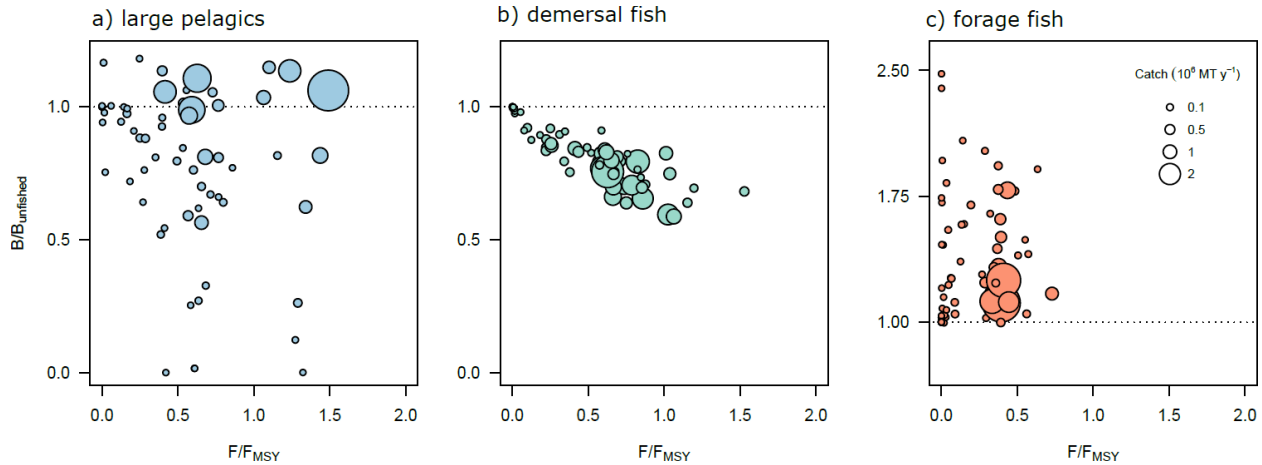
364

365 **Figure 6.** Comparison of simulated fish biomass in the unfished scenario averaged across years
 366 1961-2004 and the estimated unfished biomass (parameter K) derived from the catch-only model
 367 average across years (a). Changes in fish biomass relative to an unfished scenario between 1961
 368 and 2004 for the entire ocean (b) and all continental shelves <500 m in depth (c). Panel (a) is
 369 based on 34 LMEs for which we obtained an estimate of K for all three functional types using the
 370 catch-only model.

371

372

373



374

375 **Figure 7.** Relation between B/B_{unfished} and F/F_{MSY} for all LMEs based on average values between
 376 1990 and 2000. B_{unfished} is the biomass in an unfished scenario. The size of the dot reflects the
 377 size of the observed fishing catch.

378 **4 Discussion**

379 We estimated regional fishing exploitation levels (F/F_{MSY}) for forage, large pelagic and
380 demersal fish functional types utilizing fisheries catch and effort data. By applying the F/F_{MSY}
381 estimates in a mechanistic MEM, we successfully conducted simulations of global catches and
382 catch per functional type over time. In the FEISTY model, fishing at the estimated historical
383 exploitation rates caused a 25% decline in the biomass of large pelagic and demersal fish
384 predators and a 50% increase in forage fish biomass in shelf ecosystems over the simulated time
385 period as compared to an unfished situation. The simulated increase in forage fish biomass is the
386 result of a trophic cascade triggered by the decline of fish predators due to fishing (Frank et al.,
387 2005). The observed increase in forage fish biomass due to fishing surpasses the anticipated
388 increase of forage fish biomass due to climate change ($\pm 4\%$ fractional increase), which is
389 triggered by a decline of fish predators that suffer from higher metabolic costs in a warming
390 ocean and from declines in prey productivity (Petrik et al., 2020; Tittensor et al., 2021). These
391 findings underscore the influential role of fishing as a primary driver of fish community
392 dynamics, emphasizing the need to evaluate the impact of climate change within the context of
393 an historically altered fish community (Brander, 2007). The exploitation levels provide potential
394 standardized data forcing for simulation experiments, including model intercomparison projects,
395 where fishing effort are problematic to run, or where a common set of mortality rates across
396 MEMs is warranted.

397 Previous global simulations of fishing within the FEISTY model were kept simple by
398 implementing a constant fishing mortality rate across space and time, aiming to achieve MSY
399 across the three functional types (Petrik et al., 2019). The dynamic fishing mortality rates
400 introduced in this study improved correlations between simulated and observed catches during
401 peak exploitation (Supplementary Table S2). Part of these improvements can be attributed to
402 comparing fishing catches in all LMEs, including the lightly fished LMEs that were omitted in
403 the prior study. Without these LMEs, our correlation for forage fish (and total catch) remain
404 higher than Petrik et al. (2019) (Supplementary Table S2). This finding is in line with the re-
405 constructed F/F_{MSY} estimates which indicated that forage fish has typically faced fishing
406 mortality rates lower than F_{MSY} and are thus not fished at levels that would lead to peak
407 exploitation. Despite these improvements, a significant uncertainty persists, namely the
408 parameterization of F_{MSY} which is varying with temperature in the FEISTY model, whereas, both
409 in the FEISTY model and in nature, F_{MSY} is varying in a more dynamic way due to biotic
410 interactions within and between functional types. This dynamic nature of F_{MSY} poses a challenge
411 in capturing fishing effects in food web models (Spence et al., 2021). We recommend that other
412 MEMs approximate the temperature effect on F_{MSY} ahead of using the F/F_{MSY} estimates.

413 Among LMEs, we observe a 40% decrease in demersal fish biomass relative to unfished levels
414 with fishing rates at MSY and no clear response in forage and large pelagic fish. These effects
415 are different from what is assumed in some surplus production models where fishing at MSY is
416 estimated to cause a 50% decline in total stock biomass relative to an unfished state (Mangel,
417 2006)(chapter 6). The primary underlying factor for the complex responses in FEISTY is trophic
418 interactions. In addition, some of these dynamics can be attributed to the structural
419 characteristics of the FEISTY model. Fish in FEISTY mature at relatively small sizes compared
420 to their maximum potential size. This decision was made to encompass a spectrum of fish
421 species with just 2-3 size classes within each functional type (Petrik et al., 2019). Additionally,
422 the model includes gear selectivity parameters that target predominantly (in the case of large

423 pelagic and demersal fish) or exclusively (for forage fish) mature fishes, which allows fish to
424 survive long enough to spawn in the model. Consequently, the resilience of fish biomass to
425 fishing in FEISTY may be higher than for natural stocks and FEISTY may likely be
426 underestimating the global changes in biomass of each functional type. However, these effects
427 mainly influence biomass and less fisheries catches as gear selectivity is only expected to affect
428 the maximum sustainable yield lightly (Andersen, 2019)(fig. 5.11, see trawl selectivity).

429 Part of the observed resilience to fishing is also linked to the food web dynamics. As
430 anticipated, these dynamics increased forage fish biomass in most LMEs in the fishing scenario,
431 which is a consequence of trophic cascades initiated by the decline of demersal and large pelagic
432 fish with fishing in these systems (Andersen & Pedersen, 2010; Casini et al., 2008; Daskalov et
433 al., 2007; Frank et al., 2005). However, the food web dynamics also led to a somewhat
434 counterintuitive pattern, namely, an increase in large pelagic fish biomass with fishing in several
435 LMEs, particularly those with high observed catches. Part of this counterintuitive outcome is
436 likely a trophic cascade mediated through the larval and juvenile stages as competition with
437 demersal fish is relieved. In addition, this counterintuitive outcome is underpinned by an
438 ecological mechanism known as overcompensation (De Roos et al., 2007; Schröder et al., 2009).
439 Overcompensation entails a positive population response to mortality, which results in an
440 increased equilibrium level of the population. Overcompensation has been observed in
441 theoretical models as well as in experiments in field and laboratory systems, but only in low-
442 diversity systems (Schröder et al., 2014). Overcompensation is unlikely for large pelagic biomass
443 dynamics in diverse marine ecosystems as less fished species of similar functional type could
444 replace the more fished species.

445 Previous regional estimates of fishing exploitation used averages of assessed stocks
446 (Hilborn et al., 2020). Here we estimated exploitation patterns from aggregated catch data to
447 obtain estimates for each functional type and region. However, in natural ecosystems, a
448 functional type is exploited with a mixture of stock-specific rates, rather than one single rate, and
449 includes species without fisheries. The total catch in each functional type thus represents the
450 cumulative of all catches, potentially representing the substitution of a newly exploited stock for
451 an overexploited one. It is difficult to assess how well the catch-only model can deal with these
452 aggregated catch data as the method has solely been tested for individual stocks (Martell &
453 Froese, 2013). A comparison with regional averages of assessed stocks in our study indicated
454 that the catch-only modeled exploitation rates tend to be lower. These lower values align with
455 our expectations as stock assessment data primarily focuses on the most economically significant
456 species within each functional type, often omitting information on less commercially important
457 species that have a lower exploitation (Ovando et al., 2021). In addition, we found a large
458 difference in unfished biomass estimates between the catch-only model and FEISTY. For catch-
459 only models, the relative rates (e.g., F/F_{MSY} and B/B_{MSY}) are often considered more reliable than
460 the absolute rates of biomass, such as the carrying capacity. The catch-only carrying capacity is
461 also independently estimated for each functional type and this may cause the sum of these
462 carrying capacities to overshoot the total fish productive capacity of each ecosystem. This
463 potential overshoot of the catch-only estimates may explain why the unfished biomass estimates
464 in FEISTY are consistently lower.

465 The methodology used for deriving fishing exploitation rates, the spatial allocation
466 method, and the incorporation of mortality rates within the fish model FEISTY all introduce

467 uncertainties. These uncertainties are inherent when simulating global fish food webs and their
468 fisheries. Nevertheless, the simulated ecosystem catches demonstrated an encouraging match to
469 observed values, particularly in the case of total global catch. This alignment suggests that the
470 model reasonably captures the productive capacities of diverse ecosystems on a global scale and
471 can broadly replicate realistic long-term trends of fish catches. These results can support the
472 quantification of future trends in global fish biomass and potential fisheries production and
473 inform ongoing global assessments of climate change impacts on marine ecosystems.

474

475 **Acknowledgments**

476 We thank all ISIMIP and FishMIP coordinators for their efforts in developing and
477 maintaining the Phase3a protocol and data. We thank Matthias Büchner, Cheryl Harrison, Ryan
478 Heneghan, Derek Tittensor, Yannick Rousseau, and Olivier Maury in particular for their input
479 specific to global FishMIP models and Desiree Tommasi for her comments on the manuscript.
480 PDVD was funded by the European Union's Horizon 2020 Research and Innovation Programme
481 under the Marie Skłodowska-Curie grant agreement No 101024886. KHA acknowledges support
482 from the European Union Horizon Europe Research and Innovation Programme under project
483 NECCTON. CMP acknowledges support from NOAA grants NA20OAR4310438,
484 NA20OAR4310441, and NA20OAR4310442. JLB and CN were funded by Australian Research
485 Council project FT210100798.

486

487 **Open Research**

488 The fishing exploitation pattern time series and the FEISTY model outputs are available
489 on ZENODO (van Denderen et al., 2023). The files to run the FEISTY fish modeling simulations
490 can be found at <https://github.com/cpetrik/FEISTY/tree/master/CODE/FishMIP>. Forcing data for
491 GFDL-MOM6-COBALT is available in the ISIMIP Repository (Liu et al. 2022) and fishing
492 effort is available via Rousseau et al. (2022). Details for FishMIP-ISIMIP 3a Protocol are
493 provided here: https://github.com/Fish-MIP/FishMIP_2022_3a_Protocol

494 **References**

- 495 Adcroft, A., Anderson, W., Balaji, V., Blanton, C., Bushuk, M., Dufour, C. O., Dunne, J. P.,
496 Griffies, S. M., Hallberg, R., & Harrison, M. J. (2019). The GFDL global ocean and sea ice
497 model OM4. 0: Model description and simulation features. *Journal of Advances in*
498 *Modeling Earth Systems*, *11*(10), 3167–3211.
- 499 Andersen, K. H. (2019). *Fish ecology, evolution, and exploitation*. Princeton University Press.
- 500 Andersen, K. H., & Pedersen, M. (2010). Damped trophic cascades driven by fishing in model
501 marine ecosystems. *Proceedings of the Royal Society B: Biological Sciences*, *277*(1682),
502 795–802. <https://doi.org/10.1098/rspb.2009.1512>
- 503 Bianchi, D., Carozza, D. A., Galbraith, E. D., Guiet, J., & DeVries, T. (2023). Estimating global
504 biomass and biogeochemical cycling of marine fish with and without fishing. *Science*
505 *Advances*, *7*(41), eabd7554. <https://doi.org/10.1126/sciadv.abd7554>
- 506 Blanchard, J. L., Andersen, K. H., Scott, F., Hintzen, N. T., Piet, G., & Jennings, S. (2014).
507 Evaluating targets and trade-offs among fisheries and conservation objectives using a
508 multispecies size spectrum model. *Journal of Applied Ecology*, *51*(3), 612–622.
509 <https://doi.org/https://doi.org/10.1111/1365-2664.12238>
- 510 Blanchard, J. L., Jennings, S., Holmes, R., Harle, J., Merino, G., Allen, J. I., Holt, J., Dulvy, N.
511 K., & Barange, M. (2012). Potential consequences of climate change for primary production
512 and fish production in large marine ecosystems. *Phil. Trans. R. Soc. B*, *367*(1605), 2979–
513 2989. <https://doi.org/10.1098/rstb.2012.0231>
- 514 Blanchard, J. L., Novaglio, C., Maury, O., Harrison, C. S., Petrik, C. M., Fierro-Arcos, L. D.,
515 Ortega Cisneros, K., Bryndum-Buccholz, A., Eddy, T. D., Heneghan, R., Roberts, K.,
516 Schewe, J., Bianchi, D., Guiet, J., van Denderen, P. D., Palacios-Abrantes, J., Liu, X., ...
517 Tittensor, D. . (n.d.). *Detecting, attributing, and projecting global marine ecosystem and*
518 *fisheries change: FishMIP 2.0*.
- 519 Bouch, P., Minto, C., & Reid, D. G. (2021). Comparative performance of data-poor CMSY and
520 data-moderate SPiCT stock assessment methods when applied to data-rich, real-world
521 stocks. *ICES Journal of Marine Science*, *78*(1), 264–276.
522 <https://doi.org/10.1093/icesjms/fsaa220>
- 523 Brander, K. M. (2007). Global fish production and climate change. *Proceedings of the National*
524 *Academy of Sciences*, *104*(50), 19709–19714.
- 525 Casini, M., Lövgren, J., Hjelm, J., Cardinale, M., Molinero, J.-C., & Kornilovs, G. (2008). Multi-
526 level trophic cascades in a heavily exploited open marine ecosystem. *Proceedings of the*
527 *Royal Society B: Biological Sciences*, *275*(1644), 1793–1801.
528 <https://doi.org/10.1098/rspb.2007.1752>
- 529 Christensen, V., Coll, M., Buszowski, J., Cheung, W. W. L., Frölicher, T., Steenbeek, J., Stock,
530 C. A., Watson, R. A., & Walters, C. J. (2015). The global ocean is an ecosystem: simulating
531 marine life and fisheries. *Global Ecology and Biogeography*, *24*(5), 507–517.
- 532 Daskalov, G. M., Grishin, A. N., Rodionov, S., & Mihneva, V. (2007). Trophic cascades
533 triggered by overfishing reveal possible mechanisms of ecosystem regime shifts.
534 *Proceedings of the National Academy of Sciences*, *104*(25), 10518–10523.
535 <https://doi.org/10.1073/pnas.0701100104>
- 536 de Roos, A. M., Schellekens, T., van Kooten, T., van de Wolfshaar, K. E., Claessen, D., &
537 Persson, L. (2008). Simplifying a physiologically structured population model to a stage-
538 structured biomass model. *Theoretical Population Biology*, *73*(1), 47–62.

- 539 <https://doi.org/10.1016/j.tpb.2007.09.004>
- 540 De Roos, A. M., Schellekens, T., van Kooten, T., van de Wolfshaar, K. E., Claessen, D., &
541 Persson, L. (2007). Food-dependent growth leads to overcompensation in stage-specific
542 biomass when mortality increases: The influence of maturation versus reproduction
543 regulation. *The American Naturalist*, *170*(3), E59–E76. <https://doi.org/10.1086/520119>
- 544 FAO. (2022). *The State of World Fisheries and Aquaculture 2022. Towards Blue*
545 *Transformation*. Rome, FAO.
- 546 Frank, K. T., Petrie, B., Choi, J. S., & Leggett, W. C. (2005). Trophic cascades in a formerly
547 cod-dominated ecosystem. *Science*, *308*(5728), 1621–1623. <https://doi.org/10.1126/science.1113075>
- 548
- 549 Free, C. M., Jensen, O. P., Anderson, S. C., Gutierrez, N. L., Kleisner, K. M., Longo, C., Minto,
550 C., Osio, G. C., & Walsh, J. C. (2020). Blood from a stone: Performance of catch-only
551 methods in estimating stock biomass status. *Fisheries Research*, *223*, 105452.
552 <https://doi.org/10.1016/j.fishres.2019.105452>
- 553 Frieler, K., Volkholz, J., Lange, S., Schewe, J., Mengel, M., Rivas López, M. del R., Otto, C.,
554 Reyer, C. P. O., Karger, D. N., & Malle, J. T. (2023). Scenario set-up and forcing data for
555 impact model evaluation and impact attribution within the third round of the Inter-Sectoral
556 Model Intercomparison Project (ISIMIP3a). *EGUsphere*, 1–83.
- 557 Froese, R., Demirel, N., Coro, G., Kleisner, K. M., & Winker, H. (2017). Estimating fisheries
558 reference points from catch and resilience. *Fish and Fisheries*, *18*(3), 506–526.
559 <https://doi.org/10.1111/faf.12190>
- 560 Galbraith, E. D., Carozza, D. A., & Bianchi, D. (2017). A coupled human-Earth model
561 perspective on long-term trends in the global marine fishery. *Nature Communications*, *8*,
562 14884.
- 563 Heneghan, R. F., Galbraith, E., Blanchard, J. L., Harrison, C., Barrier, N., Bulman, C., Cheung,
564 W., Coll, M., Eddy, T. D., Erauskin-Extramiana, M., Everett, J. D., Fernandes-Salvador, J.
565 A., Gascuel, D., Guiet, J., Maury, O., Palacios-Abrantes, J., Petrik, C. M., ... Tittensor, D.
566 P. (2021). Disentangling diverse responses to climate change among global marine
567 ecosystem models. *Progress in Oceanography*, *198*, 102659.
568 <https://doi.org/10.1016/j.pocean.2021.102659>
- 569 Hilborn, R., Amoroso, R. O., Anderson, C. M., Baum, J. K., Branch, T. A., Costello, C., de
570 Moor, C. L., Faraj, A., Hively, D., Jensen, O. P., Kurota, H., Little, L. R., Mace, P.,
571 McClanahan, T., Melnychuk, M. C., Minto, C., Osio, G. C., ... Ye, Y. (2020). Effective
572 fisheries management instrumental in improving fish stock status. *Proceedings of the*
573 *National Academy of Sciences*, *117*(4), 2218–2224.
574 <https://doi.org/10.1073/pnas.1909726116>
- 575 Jacobsen, N. S., Burgess, M. G., & Andersen, K. H. (2017). Efficiency of fisheries is increasing
576 at the ecosystem level. *Fish and Fisheries*, *18*(2), 199–211.
577 <https://doi.org/10.1111/faf.12171>
- 578 Jennings, S., & Kaiser, M. J. (1998). The effects of fishing on marine ecosystems. In J.H.S.
579 Blaxter, A. J. Southward, & P. A. Tyler (Eds.), *Advances in Marine Biology: Vol. Volume*
580 *34* (pp. 201–352). Academic Press .
581 <http://www.sciencedirect.com/science/article/pii/S0065288108602126>
- 582 Liu, X., Stock, C. A., Dunne, J. P., Lee, M., Shevliakova, E., Malyshev, S., & Milly, P. C. D.
583 (2021). Simulated global coastal ecosystem responses to a half-century increase in river
584 nitrogen loads. *Geophysical Research Letters*, *48*(17), e2021GL094367.

- 585 Liu, X., Stock, C. A., Dunne, J. P., Lee, M., Shevliakova, E., Malyshev, S., Milly, P. C. D., &
586 Büchner, M. (2022): ISIMIP3a ocean physical and biogeochemical input data [GFDL-
587 MOM6-COBALT2 dataset] (v1.0). ISIMIP Repository.
588 <https://doi.org/10.48364/ISIMIP.920945>
- 589 Mangel, M. (2006). *The theoretical biologist's toolbox: quantitative methods for ecology and*
590 *evolutionary biology*. Cambridge University Press.
- 591 Martell, S., & Froese, R. (2013). A simple method for estimating MSY from catch and resilience.
592 *Fish and Fisheries*, 14(4), 504–514. <https://doi.org/https://doi.org/10.1111/j.1467->
593 [2979.2012.00485.x](https://doi.org/https://doi.org/10.1111/j.1467-2979.2012.00485.x)
- 594 Myers, R. A., & Worm, B. (2003). Rapid worldwide depletion of predatory fish communities.
595 *Nature*, 423(6937), 280–283. <https://doi.org/Doi.10.1038/Nature01610>
- 596 Ovando, D., Hilborn, R., Monnahan, C., Rudd, M., Sharma, R., Thorson, J. T., Rousseau, Y., &
597 Ye, Y. (2021). Improving estimates of the state of global fisheries depends on better data.
598 *Fish and Fisheries*, 22(6), 1377–1391. <https://doi.org/https://doi.org/10.1111/faf.12593>
- 599 Petrik, C. M., Stock, C. A., Andersen, K. H., van Denderen, P. D., & Watson, J. R. (2019).
600 Bottom-up drivers of global patterns of demersal, forage, and pelagic fishes. *Progress in*
601 *Oceanography*, 176, 102124. <https://doi.org/10.1016/j.pocean.2019.102124>
- 602 Petrik, C. M., Stock, C. A., Andersen, K. H., van Denderen, P. D., & Watson, J. R. (2020). Large
603 pelagic fish are most sensitive to climate change despite pelagification of ocean food webs.
604 *Frontiers in Marine Science*, 7, 588482.
- 605 RAM Legacy Stock Assessment Database. (2018). *Version 4.44-assessment-only. Released*
606 *2018-12-22. Accessed February 2022. Retrieved from DOI:10.5281/zenodo.2542919.*
- 607 Rousseau, Y., Blanchard, J., Novaglio, C., Kirsty, P., Tittensor, D., Watson, R., & Ye, Y. (2022).
608 *Global Fishing Effort, Institute for Marine and Antarctic Studies (IMAS), University of*
609 *Tasmania (UTAS) [data set]*, <https://doi.org/10.25959/MNGY-0Q43>.
- 610 Rousseau, Y., Blanchard, J., Novaglio, C., Pinnell, K., Tittensor, D., Watson, R., & Ye, Y.
611 (2024). A database of mapped global fishing activity, 1950- 2017'. *Scientific Data*.
612 <https://doi.org/10.1038/s41597-023-02824-6>
- 613 Schröder, A., Persson, L., & de Roos, A. M. (2009). Culling experiments demonstrate size-class
614 specific biomass increases with mortality. *Proceedings of the National Academy of*
615 *Sciences*, 106(8), 2671–2676. <https://doi.org/10.1073/pnas.0808279106>
- 616 Schröder, A., van Leeuwen, A., & Cameron, T. C. (2014). When less is more: positive
617 population-level effects of mortality. *Trends in Ecology & Evolution*, 29(11), 614–624.
618 <https://doi.org/https://doi.org/10.1016/j.tree.2014.08.006>
- 619 Spence, M. A., Thorpe, R. B., Blackwell, P. G., Scott, F., Southwell, R., & Blanchard, J. L.
620 (2021). Quantifying uncertainty and dynamical changes in multi-species fishing mortality
621 rates, catches and biomass by combining state-space and size-based multi-species models.
622 *Fish and Fisheries*, 22(4), 667–681. <https://doi.org/https://doi.org/10.1111/faf.12543>
- 623 Stock, C. A., Dunne, J. P., Fan, S., Ginoux, P., John, J., Krasting, J. P., Laufkötter, C., Paulot, F.,
624 & Zadeh, N. (2020). Ocean biogeochemistry in GFDL's Earth System Model 4.1 and its
625 response to increasing atmospheric CO2. *Journal of Advances in Modeling Earth Systems*,
626 12(10), e2019MS002043.
- 627 Stock, C. A., John, J. G., Rykaczewski, R. R., Asch, R. G., Cheung, W. W. L., Dunne, J. P.,
628 Friedland, K. D., Lam, V. W. Y., Sarmiento, J. L., & Watson, R. A. (2017). Reconciling
629 fisheries catch and ocean productivity. *Proceedings of the National Academy of Sciences* ,
630 114(8), E1441–E1449. <https://doi.org/10.1073/pnas.1610238114>

- 631 Thorson, J. T., Cope, J. M., Branch, T. A., Jensen, O. P., & Walters, C. J. (2012). Spawning
632 biomass reference points for exploited marine fishes, incorporating taxonomic and body
633 size information. *Canadian Journal of Fisheries and Aquatic Sciences*, 69(9), 1556–1568.
634 <https://doi.org/10.1139/f2012-077>
- 635 Tittensor, D. P., Novaglio, C., Harrison, C. S., Heneghan, R. F., Barrier, N., Bianchi, D., Bopp,
636 L., Bryndum-Buchholz, A., Britten, G. L., Büchner, M., Cheung, W. W. L., Christensen, V.,
637 Coll, M., Dunne, J. P., Eddy, T. D., Everett, J. D., Fernandes-Salvador, J. A., ... Blanchard,
638 J. L. (2021). Next-generation ensemble projections reveal higher climate risks for marine
639 ecosystems. *Nature Climate Change*, 11(11), 973–981. [https://doi.org/10.1038/s41558-021-](https://doi.org/10.1038/s41558-021-01173-9)
640 [01173-9](https://doi.org/10.1038/s41558-021-01173-9)
- 641 Tsujino, H., Urakawa, S., Nakano, H., Small, R. J., Kim, W. M., Yeager, S. G., Danabasoglu, G.,
642 Suzuki, T., Bamber, J. L., & Bentsen, M. (2018). JRA-55 based surface dataset for driving
643 ocean–sea-ice models (JRA55-do). *Ocean Modelling*, 130, 79–139.
- 644 van Denderen, D., Jacobsen, N., & Petrik, C. M. (2023). *Global gridded fishing exploitation*
645 *patterns (F/FMSY) of demersal and pelagic fish [Data set]. Zenodo.*
646 <https://doi.org/10.5281/zenodo.10418224>.
- 647 Watson, R. A. (2017). A database of global marine commercial, small-scale, illegal and
648 unreported fisheries catch 1950–2014. *Scientific Data*, 4, 170039.
649 <http://dx.doi.org/10.1038/sdata.2017.39>
- 650 Watson, R. A., & Tidd, A. (2018). Mapping nearly a century and a half of global marine fishing:
651 1869–2015. *Marine Policy*, 93, 171–177. <https://doi.org/10.1016/j.marpol.2018.04.023>
652